Phase transformation in a $Zr_{41}Ti_{14}Cu_{12.5}Ni_{10}Be_{22.5}$ bulk amorphous alloy upon crystallization

Wei Hua Wang,*[,1] E. Wu,[2] R. J. Wang,[1] S. J. Kennedy,[3] and A. J. Studer[3]
[1]*Institute of Physics & Center for Condensed Matter Physics, Chinese Academy of Sciences, Beijing 100080, China*
[2]*Department of Mechanical Engineering, The University of Newcastle, Callaghan, NSW 2308, Australia*
[3]*Neutron Scattering Group, Australian Nuclear Science and Technology Organization, Private Mail Bag 1, Menai, NSW 2234, Australia*

(Received 14 November 2001; revised manuscript received 29 May 2002; published 27 September 2002)

The phase precipitation, evolution, and transformation of the $Zr_{41}Ti_{14}Cu_{12.5}Ni_{10}Be_{22.5}$ bulk amorphous alloy (BAA) are investigated upon prolonged annealing by means of *in situ* neutron diffraction, x-ray diffraction, and acoustic measurements. Icosahedral quasicrystalline (*I* phase), Be_2Zr (hex, $a=0.38$ nm, $c=0.32$ nm), and Laves phase ZrTiNi are observed at the first crystallization step. The *I* phase and Be_2Zr phases transfer into stable crystalline phases at higher temperatures. The phase transitions induce marked microstructural and properties changes. The relation between the first precipitation of the temporary phases and the local microstructures of BAA is discussed. The precipitation of the *I* phase is suggested to be a structural heredity of the local icosahedral short-range order of BAA. The fundamental structural discontinuity between the crystalline and amorphous states results in an excellent glass forming ability and a high stability of the glass-forming alloy.

DOI: 10.1103/PhysRevB.66.104205 PACS number(s): 61.43.Dq, 65.40.De, 81.05.Kf

I. INTRODUCTION

Understanding the structure of amorphous alloy has been a fundamental, unsolved problem in physical and material sciences. The best approach so far, though far from complete, is to describe the amorphous alloy as a dense packing of tetrahedral building blocks. Finding a simple structural description of the amorphous alloy is a persistent challenge in condensed-matter science. Due to the small size (below the critical size for nucleation) and random orientation of the building block of the amorphous solid, the structure has remained experimentally inaccessible owing to the unavoidable averaging involved in scattering experiments, which can determine only the isotropic radial distribution function. As a consequence, the structure of amorphous alloys so far has mainly been studied by simulation.[1–6] Simulation has concluded that the face-centered-cubic structure of many crystalline solids maximizes the long-range density of closely packed spheres, and polytetrahedral packing, e.g., icosahedral packing, can maximize the short-range density of a structure.[1] It was reported recently that[7,8] the icosahedral short-range order (ISRO) is dominant in some actual amorphous alloys and even in monoatomic metallic liquids. These results have provided a better microscopic understanding of the amorphous structure, and shed light on amorphous alloy formation, melting, and supercooling. The recently developed bulk amorphous alloys (BAA's) with a high thermal stability against crystallization have offered the possibility of investigating the crystalline nucleation and growth in amorphous alloys on a long-time scale and controlled manner.[9,10] Owing to hereditable relationship between the precipitated crystalline phases of the BAA and ISRO, the study of phase precipitation and evolution during crystallization has become a promising route toward the understanding the microstructure of the BAA. However, the relation between the primary precipitation phase and short-range order has scarcely been studied, and the correlation between the microstructure and excellent glass-forming ability (GFA) of the BAA is still unclear. The primary crystallization process of amorphous alloys is not only the intermediate state on the path to the final state, but it could be the key to understanding the crystallization behavior. The properties of the temporary metastable phase can determine the subsequent growth morphology and mechanical properties. In addition, an investigation of the crystallization process is also of important for evaluating the glass-forming ability of the melts and the thermal stability of amorphous alloys. However, the crystallization process of the BAA's is very complex due to the influence of the complicated diffusion fluxes affected by the diffusional asymmetries among the different species. Even though the crystallization has been studied to a large extent, much work still needs to be done for the understanding of devitrification and phase evolution. In this work, the crystallization and phase evolution of the $Zr_{41}Ti_{14}Cu_{12.5}Ni_{10}Be_{22.5}$ BAA are investigated by *in situ* neutron diffraction, x-ray diffraction (XRD), and acoustic measurement. Our results provide evidence for the precipitation of a detectable icosahedral quasicrystalline phase (*I* phase) out of the supercooled liquid upon annealing near the calorimetric crystallization temperature in the BAA. The formed quasicrystal decomposes into several intermetallic compounds after prolonged annealing at high temperature. The density and acoustic measurements were performed to monitor the properties change during the structural evolution and transformation. The correlation between the first precipitation phases and the local microstructures is discussed. The results provide useful information for an understanding of the microstructure, the devitrification, and the properties of the excellent glass-forming alloy.

II. EXPERIMENTS

$Zr_{41}Ti_{14}Cu_{12.5}Ni_{10}Be_{22.5}$ BAA was prepared by water quenching method in a rod of 12-mm diameter; the details of

the experimental procedure can be seen in Refs. 11 and 12. The amorphous nature and homogeneity of the alloys were ascertained with XRL, differential scanning calorimetrically (DSC), and small-angle neutron scattering.[11] The glass transition temperature T_g, crystallization temperature T_x, and supercooled liquid region $\Delta T = T_x - T_g$ of the as-prepared BAA are 625, 695, and 70 K, respectively.[11] The sample rod was machined down to 10 mm in diameter and cut to a length of 10^{-1} mm for ultrasonic measurements; by grinding off the outer surface, any possible oxide materials from the quartz tube container were removed. The content was carefully checked by chemical analysis. Each end of the cylinder was polished flat and parallel. The rod sample was stepwise isothermally annealed at various temperatures in a vacuum of 10^{-3} Pa. To ensure the same thermal history the specimens were annealed up to the desired temperature using a rate of about 10 K/min, and kept in at this temperature for 2 hs. After that the sample was cooled down to room temperature quickly to keep the microstructure characteristics. After each annealing, the acoustic velocities and density were measured. The acoustic velocities were measured at room temperature by using a pulse echo overlap method.[13] The excitation and detection of the ultrasonic pulses were provided by *X*- or *Y*-cut (for longitudinal and transverse waves, respectively) quartz transducers. The ultrasonic wave are excited by the transducer, reflected from the opposite end of the BMG rod, and detected by the same transducer. The travel time of ultrasonic waves propagating through the sample with a 10-MHz frequency was measured using a MATEC 6600 ultrasonic system with a measuring sensitive of 0.5 ns. This system is capable of resolution of the velocity changes to one part in 10^5, and particularly well suitable to determination of changes in velocity.[13] The ultrasonic velocities measurement was calibrated by the known materials, such as oxide glasses.[13] The density ρ was measured by the Archimedian principle with the accuracy of 0.005 g/cm^3. The elastic constants e.g. bulk modulus *K*, and shear modulus *G* are derived from the acoustic velocities and density using conventional relations.[13] The error value for acoustic velocities are 1%,[13] and the derived values of elastic constants are estimated to be about 3%. The *in situ* neutron powder diffraction measurements were carried out on the medium-resolution powder diffractometer at the Australian Nuclear Science and Technology Organization, Lucas Heights Laboratory, using a neutron wavelength of 1.6646 Å. During the *in situ* studies, a cylinder sample of 12 mm in diameter and 20 mm high was held in the center of the neutron beam and flushed with argon gas in a medium-temperature furnace. The annealing temperature of the sample was stepped up to 873 K with a 5-h hold at each of the selected temperatures based on the DSC measurements.[11] Neutron-diffraction patterns were collected in the form of repeated scans of 1-h duration from 0° to 138° 2θ in 0.1° steps during the entire annealing experiment. XRD was conducted using a MAC *M*03 XHF diffractometer with Cu $K\alpha$ radiation.

III. RESULTS AND DISCUSSIONS

The phase sequence during the crystallization studied by *in situ* neutron diffraction is shown in Fig. 1(a). The BAA remains in an amorphous state in the lower temperature up to 623 K indicated by the diffused peaks observed from the corresponding diffraction patterns. At 673 K, some broadened peaks start to emerge on the amorphous diffused peak at around ~40°, indicating the nucleation and formation of nanosized crystalline particles. The reflections become significantly sharpened and more peaks appear at higher scattering angles at 698 K (near calorimetric T_x), and the process continues at higher temperatures up to about 723 K, suggesting that the first crystallization step is accompanied by an intensified growth of crystalline phases at this temperature range. A remarkable change in the feature of the diffraction patterns can be observed at 773–823 K [shown in Fig. 1(b)] with some peaks disappearing and some new peaks emerging, indicating a phase transition at this temperature range. The indexing of the reflection positions and the preliminary refinements of the intensities of the peaks in the diffraction patterns suggest that there are mainly three phases coexisted in the range of 675–698 K corresponding to the first crystallization step, i.e., the *I* phase, the Be_2Zr phase (hex, $a = 0.38$ nm, $c = 0.32$ nm), and a $MgZn_2$ type of Laves phase ZrTiNi ($a = 0.52$ nm, $c = 0.85$ nm); whereas at the apparent phase transition temperature (773 K) and above, the ZrTiNi Laves phase still remains, but the other two phases have

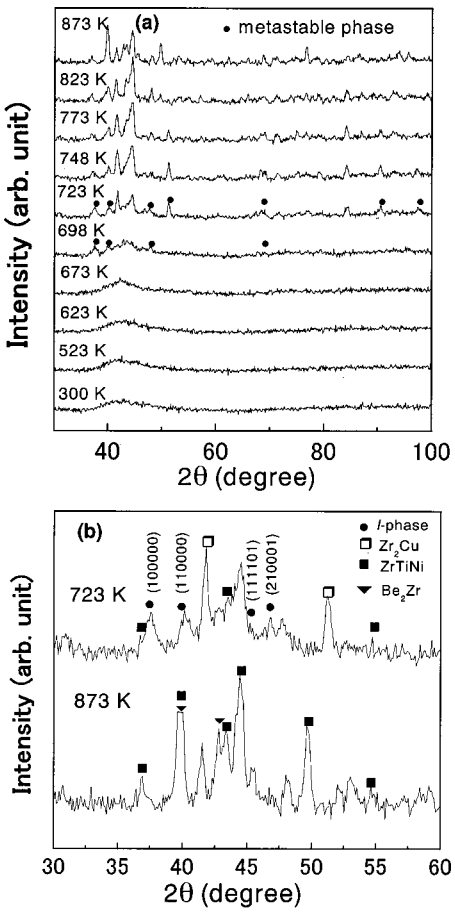

FIG. 1. (a) *In situ* neutron diffraction patterns of the BAA upon various annealing temperatures (only one pattern for each temperature is displayed in the figure). (b) The identified precipitated phases in the neutron scattering patterns of the BAA at 723 and 873 K.

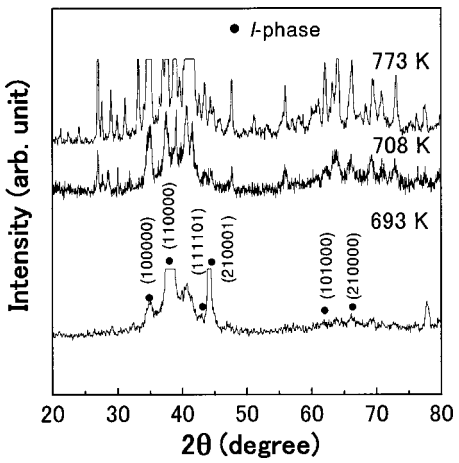

FIG. 2. The XRD pattern of the BAA at annealing temperatures shows that crystalline reflections which start to appear in 693 K disappear at higher temperature, indicating that *I* phases form during the primary crystallization process, and a metastable to stable crystalline phase transformation occurs at a high annealing temperature.

disappeared, replaced by a significant amount of Zr_2Cu phase (tetragonal, $a=0.32$ nm, $c=1.14$ nm), a small amount of Zr_2Ni phase, beryllium alloys most likely in the form of BeNi and other unidentified phases. It could be noted that there is an obvious temperature and time lag between the first emergence of the $ZrBe_2$ phase, the ZrTiNi Laves phase, and that of the *I* phases. The peaks for the *I* phase first appear at 675 K, whereas those of the $ZrBe_2$ and ZrTiNi phases appear only at later time of 698 K, indicating that the first crystallization step has proceeded in sequence for different phases. The basic (100 000) quasicrystal peak and two minor peaks at 39.8° and 45.6° hidden between those of ZrTiNi peaks can be indexed for an *I* phase of a primitive icosahedral structure with a quasilattice constant of 4.875 Å, consistent with what was observed by others.[14–16] As suggested by Eckert *et al.*,[15] this type of *I* phase is unstable and tends to transfer into the Zr_2Cu phase at above 698 K. The observations of the gradual disappearance of the *I* phase and the formation of the Zr_2Cu phase from our *in situ* neutron-diffraction studies confirm the metastable nature of the Zr-Cu-based *I* phase. The appearance of another intermediate phase of Be_2Zr in the system and its decomposition at about the same temperature as that of the *I* phase indicate that the Be_2Zr phase may have a structural similarity between the *I* phase and the hcp Be_2Zr.[17] The ZrTiNi Laves phase formed during the first crystallization step appears to be a stable crystalline phase; it accounts for nearly half of the total reflection intensity and remains relatively constant at higher temperature. XRD patterns of the BAA (shown in Fig. 2) at various annealing temperatures show a similar result to that of the neutron scattering. Some crystalline lines which correspond to the *I* phase start to appear at 693 K and disappear at higher temperature, confirming that quasicrystalline phases forms during the primary crystallization process and a metastable to stable crystalline phase transformation occurs during the crystallization process. Above 773 K, sharp Bragg peaks appear in the XRD pattern; several intermetallic compounds Zr_2Cu, Ti_2Ni, Ti_2Cu, and NiTiZr have been identified. The result agrees well with that of other researchers.[9,18]

The values of ρ, ν_l, and ν_s of the as-prepared $Zr_{41}Ti_{14}Cu_{12.5}Ni_{10}Be_{22.5}$ BMG at ambient condition are 6.125 g/cm^3, 5.174 km/s, and 2.47 km/s, respectively. *E*, *G*, *K*, and σ calculated from the acoustic data are 101.2 GPa, 37.4 GPa, 114.1 GPa, and 0.35, respectively. The obtained elastic data are in good agreement with that of the BMG measured by different methods.[9,19] σ characterizes the relative value of the compressive and shear deformation of a solid. For oxide glasses, the values of σ range from 0.15 to 0.25.[13,20] In contrast, the conventional amorphous alloys with poor GFA have higher value of $\sigma(\sigma\approx 0.40)$.[21] For the BAA, the value of σ is between that of the conventional amorphous alloys and oxide glasses. On the other hand, the GFA of the BAA (the critical cooling rate ranges from 1 to 10 K/s (Ref. 9)) is much better than that of the conventional amorphous alloys and approaches that of the oxide glasses (less than 1 K/s). The glass with small value of σ has a higher GFA, indicating that the GFA may have a correlation with the value of σ (which is close related to microstructure) in a glass-forming system. For conventional amorphous alloys, K/G is about 5.0,[21] while the K/G of the Zr-based BMG is 3.0. *G* represents the strength of the atomic interaction in a solid; the relatively larger values of *G* for the BAA means that the bond angle of the structure of the BMG cannot be changed easily. For the value of the Young's modulus *E*, the tensile fracture strength σ_f can be estimated,[22] i.e., $\sigma_f\approx E/50$; the estimated value of σ_f is about 2000 MPa, indicating that the BAA exhibits a remarkably high fracture strength.

Figures 3(a) and 3(b) exhibit the changes of ρ, longitudinal velocity ν_l, transverse velocity ν_s, and elastic constants of the BAA upon annealing. As shown in Fig. 3(a), ρ increases slightly below calorimetric T_g, and a significant increase occurs near T_g, and it reaches a maximum between T_g and T_x, indicating that larger volume change accompanies the glass transition. The density shows a continuous decrease starting at 693 K (near calorimetric T_x), obviously as a result of the precipitation of the *I* phase and other crystalline phases. The changes of ν_l and ν_s upon annealing shows a similar trend. A rapid increase in both ν_l and ν_s near T_g is a result of the glass transition, and a minimum near T_x corresponds roughly to the formation temperature of the metastable phase. At above 728 K the velocities increase rapidly again upon increasing temperature corresponding to the metastable to stable phase transformation observed during the crystallization process. ν_s has much larger relative change accompanying the phase transition in the crystallization process. The nature of the chemical bond determines the microstructure of a solid. The difference in the microstructure will influence the mechanical properties of a solid, resulting in a variation of the acoustic parameters. Therefore, the rapid changes of density and acoustic properties further confirm a drastic microstructural change during the glass transition and metastable phases to stable crystalline phase transformation. The transitions impose large physical effects on the acoustic measurements, because the acoustic properties are very sensitive to the structural change. The glass transition, precipitation, and *I* phase to stable crystalline

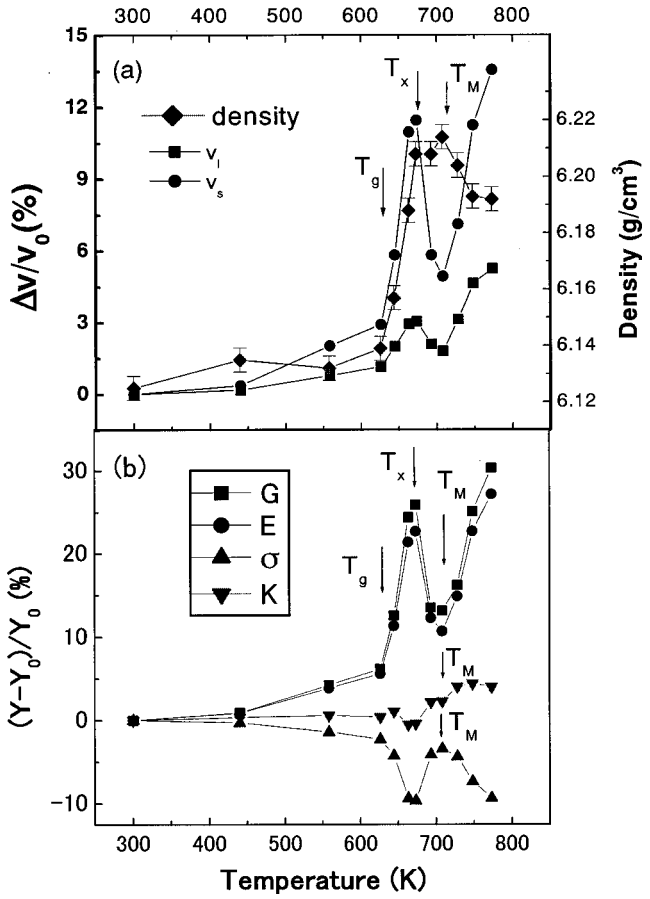

FIG. 3. (a) The variation of the density, the relative longitudinal, and transverse velocity changes with temperature, ($\nu = \nu_l, \nu_s$), ν is normalized by $\Delta\nu/\nu_0 = (\nu - \nu_0)/\nu_0$, where ν_0 is an normal velocity for as-prepared BAA. (T_g, T_x, and for metastable to stable phase transition temperature T_M are indicated in the figure). (b) The relative changes $\Delta Y/Y_0 = (Y - Y_0)/Y_0$ of variation of E, G, K and σ (Y stands for G, E, K, and σ; Y_0 stands for these in an as-prepared state) with temperature for as-prepared BAA. T_g, T_x, and T_M are indicated.

phase transformations have also been reflected in relative variations of the elastic constants G, E, K, and σ upon annealing, as shown in Fig. 3(b). G, E, K, and σ have all shown changes during transformations. G and E, which have close relations to the nature of the chemical bond, show a similar change trend with that of ν_s, and exhibit a significant increase near T_g, a steep decrease near T_x, and a marked increase after 723 K, consistent with the observed three transitions, respectively. The relative of ν_s and G changes compared to the as-prepared amorphous state for the glass transition are 13.5% and 26%, respectively; for the metastable to stable phase transition they are 8% and 17% respectively. The large relative changes of ν_s and G indicate that pronounced transverse phonon stiffness relative to the glassy state is associated with the I phase to stable intermetallic phase transition. K and σ show different change trends from those of G and E, but they clearly show kinks corresponding to the three transformations during the crystallization.

The metastable I phase was also observed in the first step of crystallization of the Zr-, Hf-, Fe-, and Pd-based BAAs; at an elevated temperature the quasicrystals transform into stable compounds.[14–17] Our result provides evidence of the precipitation of detectable I-phase clusters out of the supercooled liquid upon annealing near the calorimetric T_x in the most studied $Zr_{41}Ti_{14}Cu_{12.5}Ni_{10}Be_{22.5}$ BAA. The temporary formed quasicrystal decomposes into several intermetallic compounds after prolonged annealing at high temperature. The precipitation I phase almost is ubiquitous in the first step of the crystallization of the developed BAAs.[14–17] Questions are therefore raised: What is the relation between the precipitation of the I phase and the microstructure? How is this phenomenon correlated with the excellent GFA of an alloy? We infer that the precipitation of the I phase is a structural heredity of the local structure of the BAA. This suggests that ISRO should have existed in the as-prepared amorphous alloy. The existence of ISRO therefore provides seeds for the precipitation of the I phase and the quasicrystallinelike $ZrBe_2$ phase. It is found that the activation energy for nucleation of the I phase is smaller than that for crystallization in the ISRO, undercooling, analyzed with the classic nucleation theory.[23] Simulation with a pair potential concluded that ISRO is dominant in the undercooled alloys.[1] Chen and Spaepen[7] demonstrated that the AlMn amorphous alloy has an ISRO structure. Reichert *et al.*[8] even found direct evidence of the ISRO in a liquid Pd. All this means that the ISRO is actually one of popular building blocks in condensed matter.

The stoichiometry of many quasicrystalline phases is governed by the Hume-Rothery rule,[24,25] placing the Fermi level into a minimum of the electronic density of states. That is, a quasicrystalline state is stabilized when the number of conductive electrons per atom (e/a) is such that the Fermi surface is located in the vicinity of the pseudo-Brillouin-zone boundary. In such a case, $k_p \approx 2k_f$, where k_f is the momentum of electron at the Fermi level and k_p is the width of the pseudo-Brillouin-zone. It is interesting to reveal that if the Hume-Rothery nature can be brought forward for the bulk amorphous alloy. To do this, it is assumed that the amorphous alloy has a spherelike Fermi surface, which will touch the spherelike pseudo-Brillouin-zone boundaries in all direction.[26] The zone of a Fermi radius with a charge of e/a can roughly be described by a free-electron model, $k_f = (3\pi^2 N)^{1/3}$, where N is the valence electron concentration per unit volume and can be calculated as.[27,28] $N = (e/a) \times (A\rho/M)$. Here ρ is the density of the BAA, A is the Avogadro constant, and M is the average atomic weight. By using the valence electron contributions proposed by Mayer *et al.*[29] with 1.1 for Zr, -1 for Ni, $+1$ for Cu, 1.1 for Ti, and 2 for Be, the average e/a of the BAA is calculated as 1.08, and $k_f = 12.5\ \mathrm{nm}^{-1}$. These result in a pseudo-Brillouin zone of the BAA as of $k_p \approx 2k_f = 25.0\ \mathrm{nm}^{-1}$. Based on an *in situ* neutron-diffraction observation, the diffused scattering peak of the BAA and the strongest characteristic scattering peak (110 000) of the precipitation quasicrystals is located at about $k_p = 26.0$ and $k_p = 25.8\ \mathrm{nm}^{-1}$, respectively (the reciprocal vector defining bisecting faces of the Brillouin zone corresponds to the sharpest diffraction peak in diffraction patterns, $k_p = 4\pi \sin\theta/\lambda$). The calculated value is coincident well with the short-range order of the BAA. This indicates that the

Zr-based BAA is a Hume-Rothery phase satisfying the relation $k_p \approx 2k_f$, and strongly related to the quasicrystalline phase in its electronic structure. The authors of Ref. 27 found that the composition which has the best GFA in the ZrAlNiCu quaternary phase diagram fall in a constant e/a area similar to the e/a constant theory found in quasicrystalline systems.[24,25] Nagel and Tauc[28] also reported that other amorphous phases could be stabilized when they were Hume-Rothery phases. The similarity of the amorphous phase and the *I* phase in an electric structure leads to a speculation that a similarity also exists in their atomic structures. The initial precipitation of the *I* phase and its similar electric structure with that of the BAA indicates the existence of ISRO in the local atomic configuration of the BAA. This suggestion would provide a reasonable explanation to the excellent GFA of the BAA. Conventional amorphous alloys with a poor GFA have corresponding crystalline compounds similar to the amorphous alloys in their local structures and compositions.[2] For these alloys, the cooling rate has been the most important factor in inhibiting the nucleation and growth of the competing crystalline phases. For the BAA, however, the critical cooling rate has been much lower, and their local microstructural characterization therefore becomes a decisive factor for its glass-forming ability. The ISRO in the amorphous state would provide an additional barrier for the nucleation of the crystalline phases, since the *I* phase, with fivefold rotational symmetry, would be incompatible with the translational symmetry of normal crystalline phases; it has to be dissociated before the solidification of the crystalline phases could occur. From a kinetic point of view, the crystallization of the BAA requires a substantial redistribution of the component elements across the icosahedral liquid. The highly dense, randomly packed, structure of the BAA in its supercooled state results in an extremely slow atomic mobility.[30] Thus it makes the redistribution of atoms on a large range scale very difficult. This fundamental structural discontinuity between the crystalline and the amorphous state suppresses the nucleation and growth of the crystalline phase from the supercooled liquid and results in an excellent GFA.

IV. CONCLUSIONS

The crystallization of the $Zr_{41}Ti_{14}Cu_{12.5}Ni_{10}Be_{22.5}$ BAA, characterized by a detectable precipitation of a metastable quasicrystalline phase at the first crystallization step, and by a further transition to stable crystalline phases at high temperature, accompanied by induced microstructural and property changes, has been observed. A Brillouin-zone analysis, applying a free-electron model, indicates the Zr-based BAA is a Hume-Rothery phase satisfying the relation $k_p \approx 2k_f$, and has an electron structure similar to that of the *I* phase. The precipitation of the *I* phase is suggested to be a structural heredity of ISRO. The fundamental structural discontinuity between the crystalline and amorphous states results in the excellent glass-forming ability of the glass-forming alloy.

ACKNOWLEDGMENTS

The authors are grateful for the financial support of the National Natural Science Foundation of China (Grant Nos. 59925101 and 5003010). Fruitful discussion with Dr. M. X. Pan, and the sample preparation assistance from D. Q. Zhao and L. L. Li are greatly appreciated.

*Corresponding author. Email address: whw@aphy.iphy.ac.cn

[1] D. M. Herlach, Mater. Sci. Eng. **R12**, 177 (1994).
[2] R. Wang, Nature (London) **278**, 700 (1979).
[3] L. F. O. Rodriqueze and J. M. Soler, Phys. Rev. Lett. **81**, 3159 (1998).
[4] J. D. Bernal, Nature (London) **185**, 68 (1960).
[5] H. Schumacher, U. Herr, D. Oelgeschlaeger, A. Traverse, and K. Samwer, J. Appl. Phys. **82**, 155 (1997).
[6] A. P. Amarillas and I. L. Garzon, Phys. Rev. B **53**, 8363 (1996).
[7] L. C. Chen and F. Spaepen, Nature (London) **336**, 366 (1988).
[8] H. Reichert *et al.*, Nature (London) **408**, 839 (2000).
[9] W. L. Johnson, Mater. Sci. Forum **225–227**, 35 (1996).
[10] A. Inoue, Mater. Trans., JIM **36**, 866 (1995).
[11] W. H. Wang and H. Y. Bai, J. Appl. Phys. **84**, 5961 (1998).
[12] W. H. Wang, Q. Wei, and H. Y. Bai, Appl. Phys. Lett. **71**, 58 (1997).
[13] D. Schreiber, *Elastic Constants and Their Measurement* (McGraw-Hill, New York, 1973); R. J. Wang, F. Y. Li, J. Xu, and H. S. Xie, J. High Press. Phys. **8**, 177 (1994) (in Chinese).
[14] T. Zhang, A. Inoue, M. Matsushita, and J. Saida, J. Mater. Res. **16**, 20 (2001).
[15] J. Eckert, N. Mattern, M. Zinkevitch, and M. Seidel, Mater. Trans., JIM **39**, 623 (1998).
[16] N. Wanderka, M. P. Macht, M. Seidel, S. Mechler, K. Stahl, and J. Z. Jiang, Appl. Phys. Lett. **77**, 3935 (2000).
[17] C. Li and A. Inoue, Phys. Rev. B **63**, 172201 (2001).
[18] J. G. Wang, B. W. Chai, T. G. Nieh, and T. C. Liu, J. Mater. Res. **15**, 913 (2000).
[19] R. D. Conner, R. B. Dandliker, and W. L. Johnson, Acta Mater. **46**, 6089 (1998).
[20] K. Kondo, S. Lio, and A. Sawaoka, J. Appl. Phys. **52**, 2826 (1981).
[21] H. S. Chen, J. T. Krause, and E. Coleman, J. Non-Cryst. Solids **18**, 157 (1975).
[22] H. S. Chen and T. T. Wang, J. Appl. Phys. **41**, 5338 (1970).
[23] D. Holland-Moritz, D. M. Herlach, and K. Urban, Phys. Rev. Lett. **71**, 1196 (1993).
[24] J. Friedal and F. Denoyer, Acad. Sci., Paris, C. R. **305**, 171 (1987).
[25] V. G. Vaks, V. V. Kamyshendo, and G. D. Smolyuk, Phys. Lett. A **132**, 131 (1988).
[26] P. Haussler, Z. Phys. B: Condens. Matter **53**, 15 (1983).
[27] C. H. Shek, Y. M. Wang, and C. Dong, Mater. Sci. Eng., A **291**, 78 (2000).
[28] S. R. Nagel and J. Tauc, Phys. Rev. Lett. **35**, 380 (1975).
[29] D. Mayer, F. Cyroy-Lackmann, G. Trambley de Laissardiere, and T. Klein, J. Non-Cryst. Solids **153–154**, 412 (1993).
[30] W. H. Wang, Q. Wei, and S. Friedrich, Phys. Rev. B **57**, 8211 (1998).